

Model Based PI Controller Design and Test of a DC Motor Using Root Locus

Ulas Beldek¹, Ahmed Imad Mahmood²

¹(Mechatronics Engineering Department/ Cankaya University, Turkey)

²(Electronics and Communication Engineering Department/ Cankaya University, Turkey)

Corresponding Author: Ulas Beldek

Abstract: In this paper the mathematical model of an experimental DC motor control system is constructed in a simulative environment for speed (angular velocity) control process and a PI controller is designed using root locus technique. The designed controller is then tested in different scenarios with varying reference signals and changing disturbance load conditions. The designed controller demonstrated satisfactory results in simulations.

Keywords –DC Motors, Control Theory, Angular Velocity Control, PI Controllers, Root Locus,

Date of Submission: 25-04-2019

Date of acceptance: 05-05-2019

I. INTRODUCTION

Electrical motors are one of the main devices used for electromechanical energy conversion. Establishing experimental set-ups that enables implementation and testing of different control applications over these devices is important to increase their practical usage and efficiency.. One of the most important applications electrical motors are used for is adjusting the speed of them for driving a load at desired conditions. Speed control of motors faces with various sorts of difficulties such as precision [1] and applicability in altering load conditions [2] hence the design of the speed control system for motors should cope with such challenges. Many control procedures and algorithms are implemented to deal with these challenges: fuzzy logic [3, 4, 5, 6, 7] neural-networks [8, 9] and machine learning and optimization [10, 11, 12, 13] tools are also applied for this purpose. However, these tools most of the time require some appropriate experimental data about the system be controlled and before applying them to the real time system some adjustments due to the system model is still necessary. Hence a model-based control is still favorable. One of the most convenient and favored control settlements to handle the challenges in control applications is proportional-integral-derivative (PID) control [14]. PID controllers are widely used for speed control of electrical motors [15]. This algorithm is highly preferred as its implementation is easy and it usually meets the requirements corresponding to the control application by suitable choice of parameter setting. If the PID controller parameters are selected appropriately, the requirements in the speed control such as tracking different types of reference input signals properly in a short period of time with conceivable smallest overshoot and also with the minimum steady-state error value can be quickly achieved with high efficiency. Additional mathematical technique can also assist to determine the parameters of PID controllers. One of these techniques is called as root locus [16, 17]. The technique uses a mathematical function analysis background in order to designate the locations of the closed loop poles of a linear system (or linearized system at the operating point), which is represented by an open loop transfer function. It is a graphical technique for testing how the roots of a linear systems' characteristic equation changes with changing system parameters. In addition if it is coupled with PID controller root locus can also be used to set controller parameters as well [7]. Thus root locus can be engaged to improve the system performance in control applications and hence it enables the engineers to stabilize and control the systems outputs. In this study, the intention is devising a suitable controller structure that is fruitful in DC motor speed control application in simulation environment. Primarily, the mathematical model of a DC motor speed control system for of a laboratory experiment set-up is constructed in simulation. The model then is used to obtain a controller structure. To enable the controller with specific properties such as having less steady-state error and less overshoot, root locus technique is appealed. The designed controller is then tested in different simulation scenarios with differing reference signal and disturbance load conditions and its capacity is experienced. The main contribution of this study is that a preparatory simulative motor speed control application is carried out before a real time implementation and the potential of the simulated controller is tested in many different reference signal and disturbance load scenarios. The results show that designed controller structure by root locus technique both operates properly at differing reference signals and it can deal with differing load conditions. In section 2 the DC motor and corresponding speed control system are described and their mathematical simulation models are obtained. In section 3, a PI controller is developed using root locus of the mathematical model

obtained in section 2. In section 4, the designed PI controller is tested in different scenarios. Section 5 gives the concluding remarks and future works.

II. DC MOTOR CONTROL SYSTEM

The DC motor control system used in this study is owned by Feedback Instruments [18]. The electrical parts of the control system convert the observed mechanical entities to electronic signals. These electrical signals are then transferred to the computer via an I/O card. The mathematical model of the whole system can be described by equations governing both mechanical and electrical parts of the motor. Basically, for a DC motor, the torque induced over the motor is proportional with the current passing from the electrical part:

$$\tau = K_t I \quad (1)$$

In (1) K_t is the torque constant for the DC motor, I is the current passing from the electrical part and τ is the induced torque. Similarly, the back electromotive force induced over the electrical part is proportion with the angular velocity of the shaft of the motor:

$$V_{emf} = K_b \cdot \dot{\theta} \quad (2)$$

In (2), the induced electromotive force is V_{emf} , the electromotive force constant of the motor is K_b , the angular velocity of the shaft is $\dot{\theta}$. Using Newton's law, the mechanical equation can be written:

$$J\ddot{\theta} = -d\dot{\theta} + \tau - \tau_{ext} = -d\dot{\theta} + K_t \cdot I - \tau_{ext} \quad (3)$$

In (3) d is a linear the viscous friction coefficient, J is the moment of inertia of the and $\ddot{\theta}$ is the angular acceleration of the motor. τ_{ext} in the equation represents the external disturbance torque due to load. Similarly, the electrical dynamic equation of the motor can be written:

$$V_m - V_{emf} = L \frac{dI}{dt} + R \cdot I \quad (4)$$

In (4) V_m is Voltage applied to the armature, L is the inductance value of the armature R is the internal resistance of the armature. Using (2) and (4), (5) is obtained:

$$V_m = L \frac{dI}{dt} + R \cdot I + K_b \cdot \dot{\theta} \quad (5)$$

(3) and (5) can be reorganized and the state space representation for the system can be obtained:

$$\frac{d}{dt} \begin{bmatrix} \dot{\theta} \\ I \end{bmatrix} = \begin{bmatrix} -\frac{d}{J} & \frac{K_t}{J} \\ -\frac{K_b}{L} & -\frac{R}{L} \end{bmatrix} \cdot \begin{bmatrix} \dot{\theta} \\ I \end{bmatrix} + \begin{bmatrix} 0 \\ 1 \end{bmatrix} \cdot V_m + \begin{bmatrix} -1 \\ 0 \end{bmatrix} \cdot \tau_{ext} \quad (6)$$

The derivative of the angular position θ is equal to angular velocity w :

$$\dot{\theta} = w \quad (7)$$

There are also conversion devices such as amplifiers to amplify the signal coming from the computer (between 2.5 Volt and -2.5 Volt) to levels that can be employed to the motor (between 24 Volt and -24 Volt) and this conversion ratio is 9.6. If the input signal coming from the computer is u then the motor armature voltage can be calculated simply using:

$$V_m = 9.6 \times u \quad (8)$$

Hence, the state-space representation using (8) becomes:

$$\frac{d}{dt} \begin{bmatrix} W \\ I \end{bmatrix} = \begin{bmatrix} -\frac{d}{J} & \frac{K_t}{J} \\ -\frac{K_b}{L} & -\frac{R}{L} \end{bmatrix} \cdot \begin{bmatrix} W \\ I \end{bmatrix} + \begin{bmatrix} 0 \\ 9.6 \end{bmatrix} \cdot u + \begin{bmatrix} -1 \\ 0 \end{bmatrix} \cdot \tau_{ext} \quad (9)$$

The output of the system is angular velocity (a conversion is necessary from rad/sec to rot/min by multiplying with a factor of $\frac{60}{2\pi}$):

$$y = \begin{bmatrix} \frac{60}{2\pi} & 0 \end{bmatrix} \cdot \begin{bmatrix} W \\ I \end{bmatrix} \quad (10)$$

Using (9) and (10), the transfer function of the system can be obtained:

$$G(s) = \frac{Y(s)}{U(s)} = \frac{K_{add} \times K_t}{s^2 + \frac{(R+dL)}{JL}s + \frac{dR+K_b K_t}{JL}} \quad (11)$$

$Y(s)$ is the Laplace form of output angular velocity signal (in rot/min) and $U(s)$ is the Laplace form of the input voltage signal u (in Volt) and K_{add} is the additional gain value coming from the amplifiers and conversion from rad/sec to rot/min which is given by the:

$$K_{add} = \frac{60 \times 9.6}{2\pi} \quad (12)$$

The parameters of the DC motor are given in Table 1 (these parameters are taken from [18]).

Table 1: DC motor parameters

Parameter	Value
J-moment of inertia	$140 \times 10^{-7} \text{ Kg.m}^2$
K_t -torque constant	0.052 Nm/A
K_b -electromotive force constant	0.057 Vs/rad
d-linear approximation of viscous friction	10^{-6} Nms/rad
R-resistance	2.5 Ω
L-inductance	2.5 mH

Using (9), a SIMULINK model of the DC motor is obtained as in Fig. 1

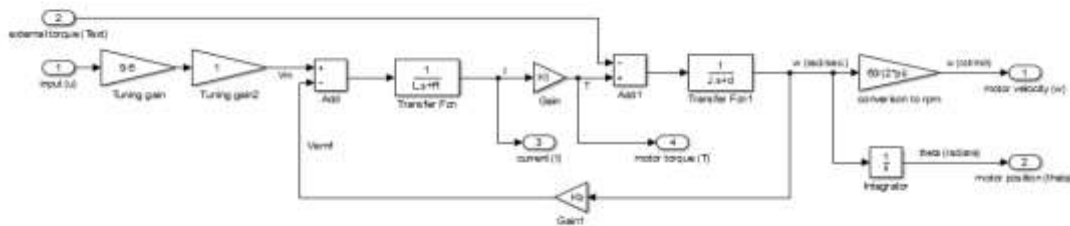


Figure 1: DC motor model.

The model in Fig.2 is converted into a sub-system block as in Fig. 2.

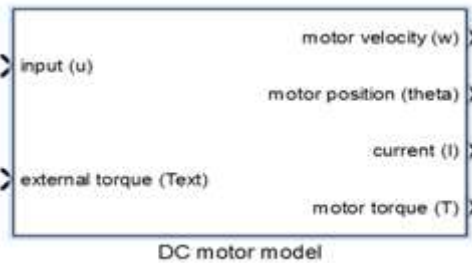


Figure 2: The sub-block for the DC motor model

It is intended to control the DC motor for speed (angular velocity) control process using a PI (proportional+integral) controller. The transfer function of PI controller is given by:

$$C(s) = P + \frac{I}{s} + Ds \quad (13)$$

It is widely used in control applications. However its parameters should be adjusted intelligently to achieve noble performance. In Fig. 3 the model of the whole control system where a PI controller is also inserted for speed control process is shown.

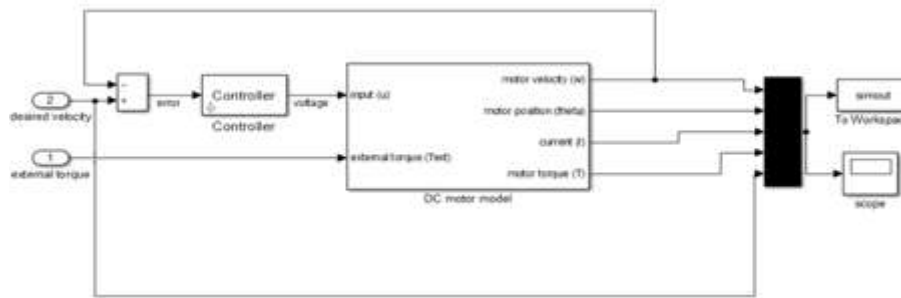


Figure 3: Model for DC motor speed control process

III. CONTROLLER STRUCTURE

The mathematical model of the DC motor system is employed in order to devise a suitable controller structure for angular velocity control process. For this purpose parameters in Table 1 are employed in (11) and, the transfer function of the open loop system is obtained:

$$G(s) = \frac{1.362 \times 10^8}{s^2 + 1000s + 8.476 \times 10^4} \quad (13)$$

The root locus of the open loop system given in (13) is drawn in Fig. 4.

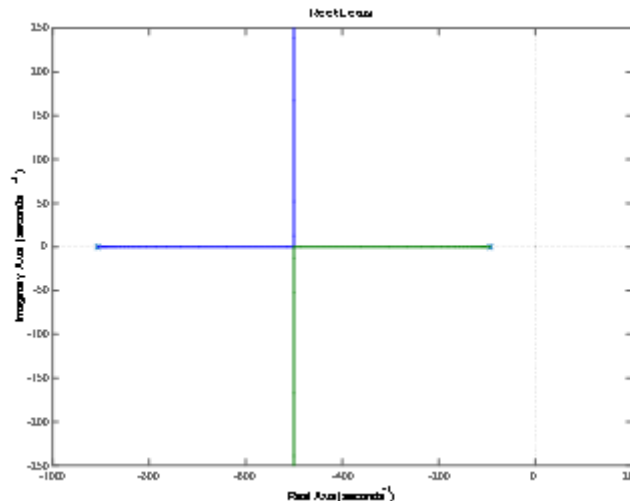


Figure 4: Root locus of the open loop system in (13).

The root locus plot helps determining the control strategy. The open loop system originally has two poles and no zeros and the poles are both on the left open half plane and hence the system is still stable. However to obtain promising performance criteria such as less maximum overshoot and minimal steady state error, feedback control with a suitable controller structure is necessary. Solely application of a small P (proportional) control might cause a steady state error value. If the gain value of the P controller is further increased steady-state error can be decreased, however at this case it is possible to observe an overshoot at the output since the poles of the root locus plot possesses imaginary parts in case the proportional gain value exceeds a critical level. For these reasons it is more preferable to use a PI (proportional integral) compared to P controller. A PI controller exhibits nearly zero steady state error due to application of a unit step change in the reference set value as the transfer function at (13) is zero-type (it does not has a pole at the origin). The structure of the PI controller is of the form:

$$C(s) = P + \frac{I}{s} \quad (14)$$

P is the proportional gain and I is the integral gain values. With a mathematical transformation (14) can be rewritten:

$$C(s) = P \times \frac{s+P}{s} \quad (15)$$

PI controller is indeed depicted as a sub-system having a single pole at the origin and a zero at the left open half plane. P and I parameters should be determined such that the controller has the desired zero location to eliminate the effect of dominant pole of the original system and necessary gain value to relocate the closed loop

system poles. The poles of the original system are located at -906.5804 and -93.4910. Hence, the zero of the controller should be located to -93.4910 to suppress the dominant pole of the original system. To accomplish this, the integral and proportional gain ratios should be:

$$\frac{I}{P} = 93.4910 \quad (16)$$

Using (13) (15) and (16) transfer function T(s) is obtained which is the open loop transfer function of the controlled system by the PI controller:

$$T(s) = C(s) \times G(s) = P \times \frac{1.362 \times 10^8 s + 1.273 \times 10^{10}}{s^3 + 1000 s^2 + 8.476 \times 10^4 s} = P \times G_o(s) \quad (17)$$

For T(s), P is now the free gain parameter and adjusting the value of P is very easy by considering the root locus plot of G_o(s):

$$G_o(s) = \frac{1.362 \times 10^8 s + 1.273 \times 10^{10}}{s^3 + 1000 s^2 + 8.476 \times 10^4 s} \quad (18)$$

In Fig. 5 the root locus plot of G_o(s) is given

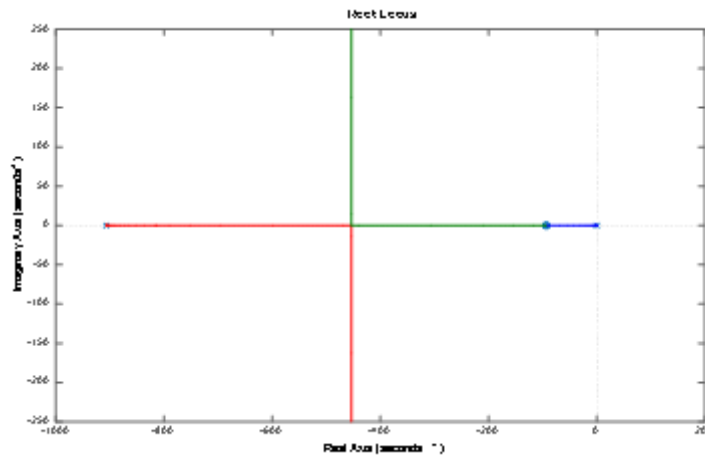


Figure 5: Root locus plot of (18).

If the gain value is taken as 0.00151 then the closed loop poles of G_o(s) coincides at the location -453 and they do not have any imaginary parts hence due to a unit step reference input no overshoot is assumed to be possible. Hence, the P parameter of PI controller is taken as 0.00151. Using (16) and taking P as 0.00151, I value can be computed as 0.1412. Finally the final PI controller structure is obtained:

$$C(s) = 0.00151 + \frac{0.1412}{s} \quad (19)$$

IV. TESTS

Using this controller structure in (19) the feedback system in Fig. 4 is simulated for unit step change in reference signal (from 0 rot/min to 400 rot/min) and the corresponding voltage (control signal), velocity (angular velocity), position and current profiles in Fig. 6 are obtained

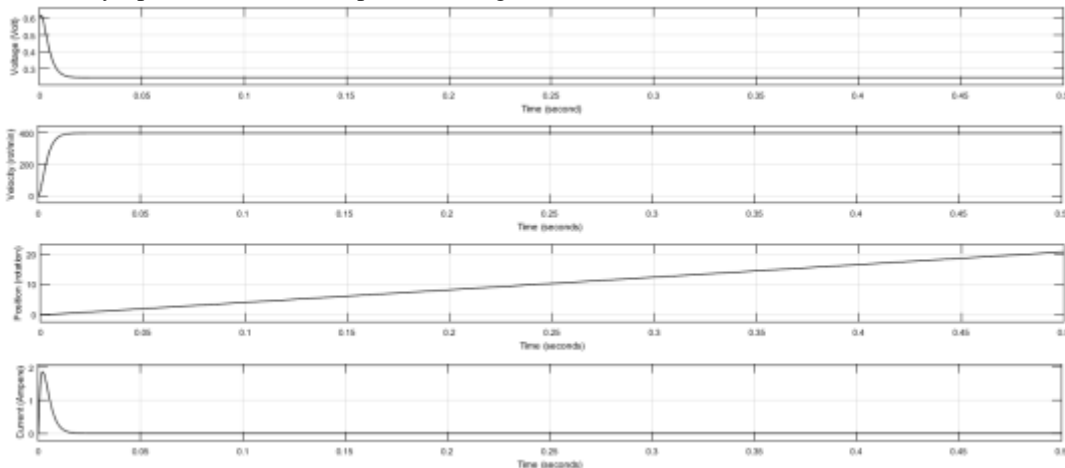


Figure 6: Voltage, velocity, position and current profiles for tracking unit step reference signal of 400 rot/min.

The controller works very well for unit step change in reference signal when there are no external disturbances. The steady state error value is zero, there is no overshoot, and oscillations are not observed at the output. Besides the input voltage applied to the motor is not exceeding the limits and hence the controller works successfully under no load conditions. Next step is to test the performance of the controller with several reference signals at various load conditions (external disturbance). Firstly a load that provides pulse like external torque of 0.1 Newton-meter between first and second seconds is simulated when there is unit step change in reference signal (from 0 rot/min to 400 rot/min). In Fig. 7 simulation results are given. The results indicate that the angular velocity of the motor returns to the reference set value of 400 rot/min very rapidly besides no steady state error is observed. The current and applied voltage values are also in the desired ranges.

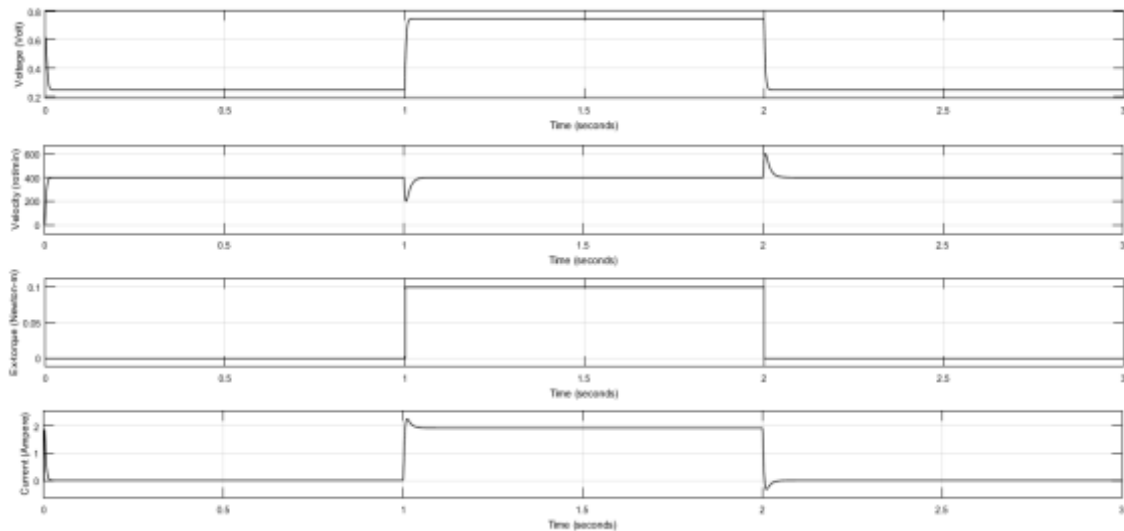


Figure 7: Voltage, velocity, external torque and current profiles for unit step reference signal tracking of 400 rot/min in case of pulse type external torque

Secondly as an alternative application, the reference signal is changed. It is taken as combination of different sinusoidal and a random signal. This signal is given by the formula:

$$r(t) = 200 \times \sin(2t) + 150 \times \sin(0.1t) + 400 \times (0.33t) + 1000 \times p(t) \text{ (rot/min)} \quad (20)$$

In (20), $r(t)$ is the reference signal and $p(t)$ is a random signal sampled at every 5 seconds whose mean value is 0 and variance value is 0.02. Due to its sampling, random signal $p(t)$ creates some discontinuities (jumps) at $r(t)$. $r(t)$ is shown in Fig. 8.

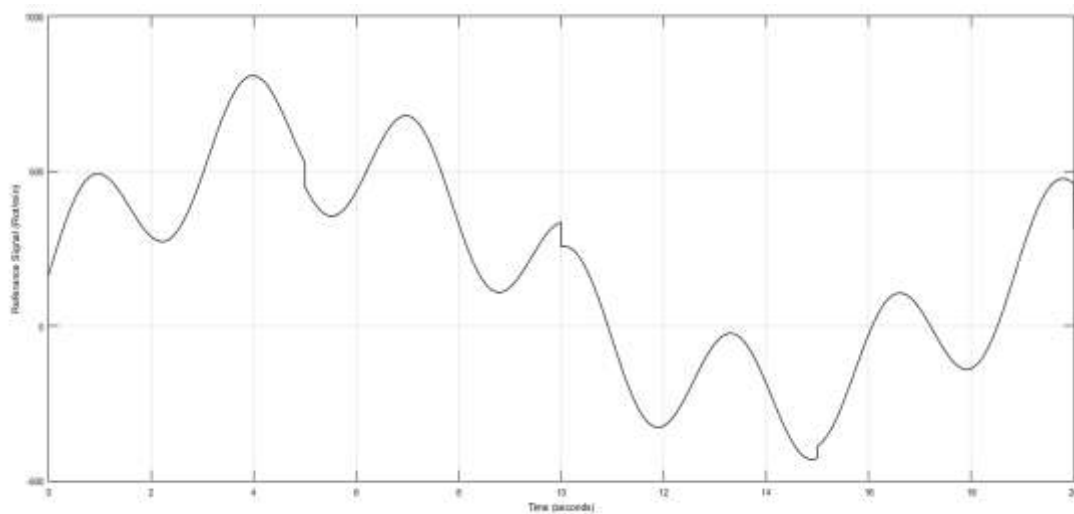


Figure 8: Reference angular velocity signal given in (20)

Applying the reference signal in Fig. 8 coupled with a pulse type external Torque of 0.1 Newton-meter that is valid between 8th and 10th seconds the controlled system produced the following angular velocity in Fig. 10. For comparison the reference signal is also drawn together with the angular velocity in Fig. 9.

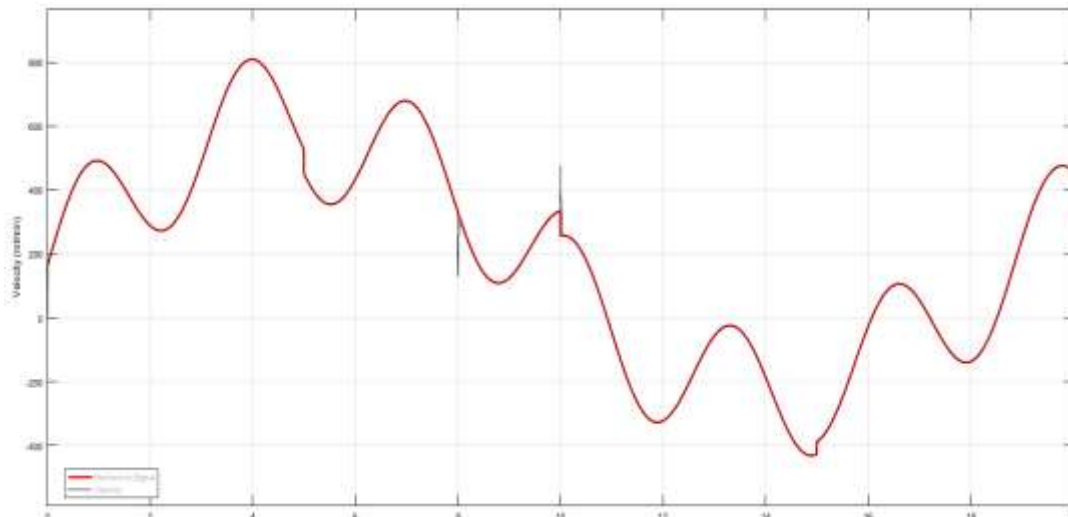


Figure 9: Angular velocity and reference signal in (20) drawn together as pulse type external torque is applied.

In Fig. 10, the voltage, angular velocity, external torque and the current profiles are given.

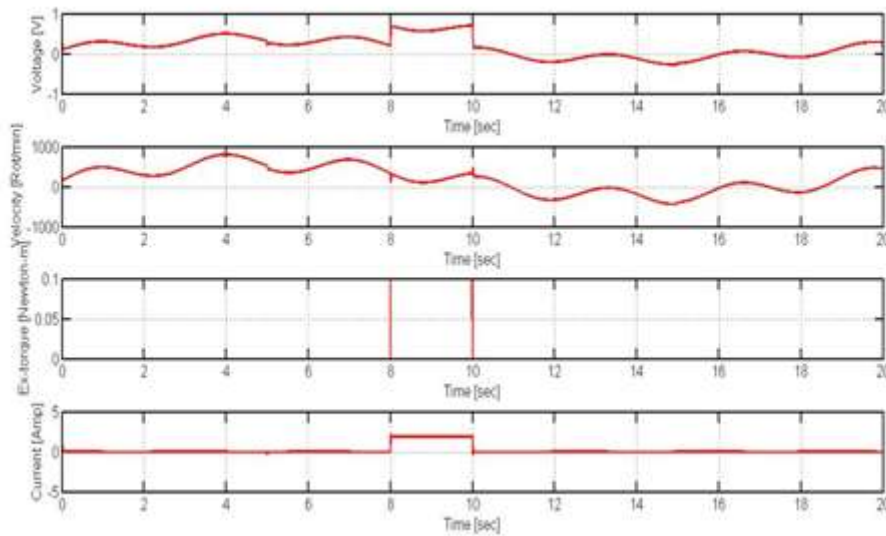


Figure 10: Voltage, angular velocity, torque and current profiles when pulse type external torque is applied while tracking the reference signal given in (20).

In the presence of even sinusoidal reference signal and pulse like external torque the controller performance is still very well. Thirdly as another application, the effect a sinusoidal disturbance coupled with the reference signal given in 20 is monitored. The sinusoidal disturbance due to external torque is given by:

$$T_{\text{external}} = \begin{cases} 0 \text{ Newton - meter, } t \leq 10 \text{ seconds} \\ 0.1 + 0.1 \times \sin(2\pi t) \text{ Newton - meter, } t > 10 \text{ seconds} \end{cases} \quad (21)$$

This simulation is run for 20 seconds and corresponding voltage, external torque, velocity and current profiles shown in Fig. 11 are obtained.

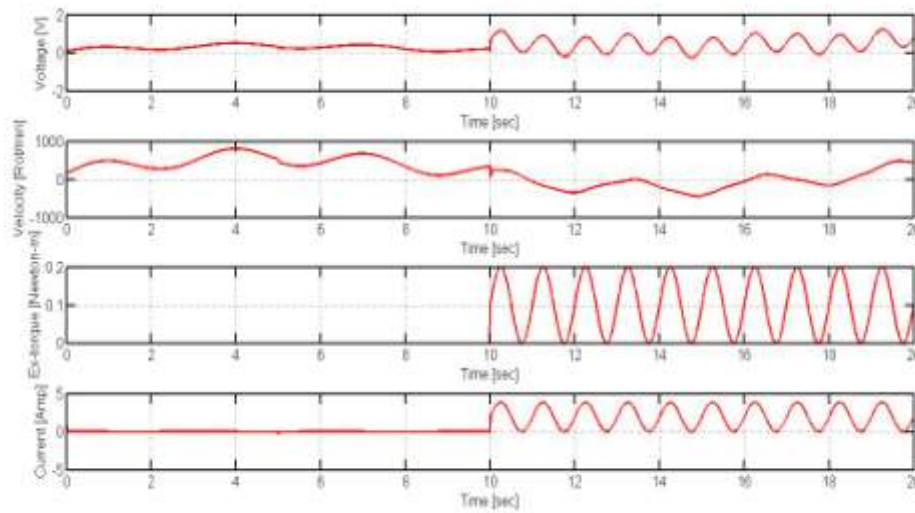


Figure 11: Voltage, velocity, external torque and current profiles for sinusoidal reference signal tracking when external torque in (21) is applied

In order to see the effect of sinusoidal torque for reference tracking, the reference signal and obtained angular velocity are drawn together in Fig. 12.

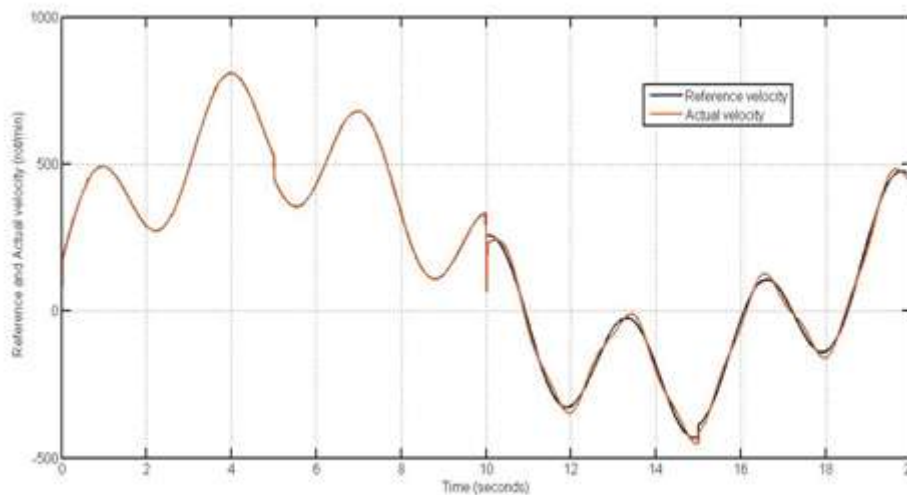


Figure 12: Velocity profile for sinusoidal reference signal tracking when external torque in (21) is applied

Even in case of sinusoidal disturbance the designed controller is able track the reference signal. Additionally, we want to see the effect of increasing the frequency and the amplitude of the disturbance signal. First we increased the frequency of the disturbance signal (it is increased from 1 Hertz to 2 Hertz) while leaving the amplitude unchanged. Hence, the new external disturbance is taken as:

$$T_{\text{external}} = \begin{cases} 0 \text{ Newton - meter, } t \leq 10 \text{ seconds} \\ 0.1 + 0.1 \times \sin(4\pi t) \text{ Newton - meter, } t > 10 \text{ seconds} \end{cases} \quad (22)$$

Obtained reference signal and angular velocity profiles are given in Fig. 13.

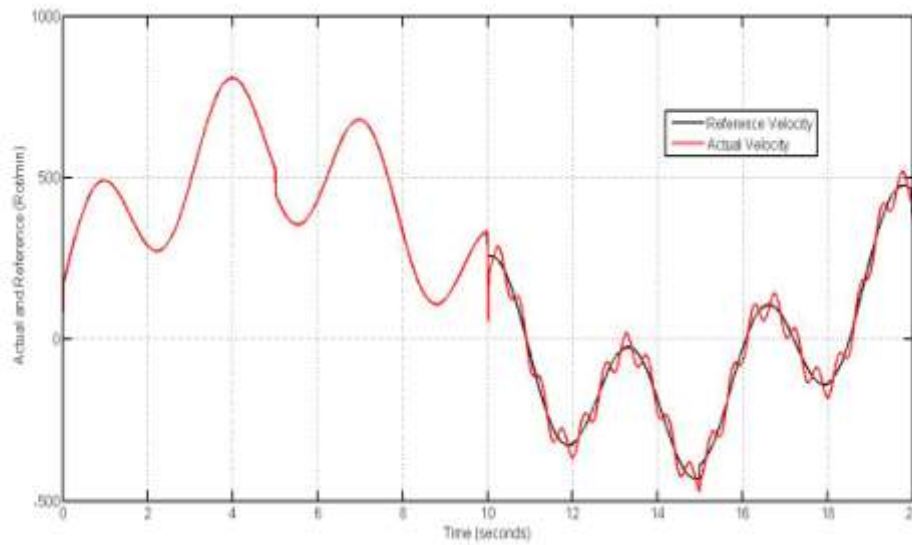


Figure 13: Effect of changing the external disturbance as in (22) for sinusoidal reference signal tracking

Increasing the frequency spoils the performance slightly however the reference signal is followed still satisfactorily. Effect of amplitude change for reference signal tracking is also monitored. This time the external disturbance is taken as:

$$T_{\text{external}} = \begin{cases} 0 \text{ Newton – meter, } t \leq 10 \text{ seconds} \\ 0.2 + 0.2 \times \sin(2\pi t) \text{ Newton – meter, } t > 10 \text{ seconds} \end{cases} \quad (23)$$

The frequency of the sinusoidal term in (23) is taken as 1 Hertz however the amplitude is taken as 0.2. The reference signal and the actual velocity profiles are shown in Fig. 14.

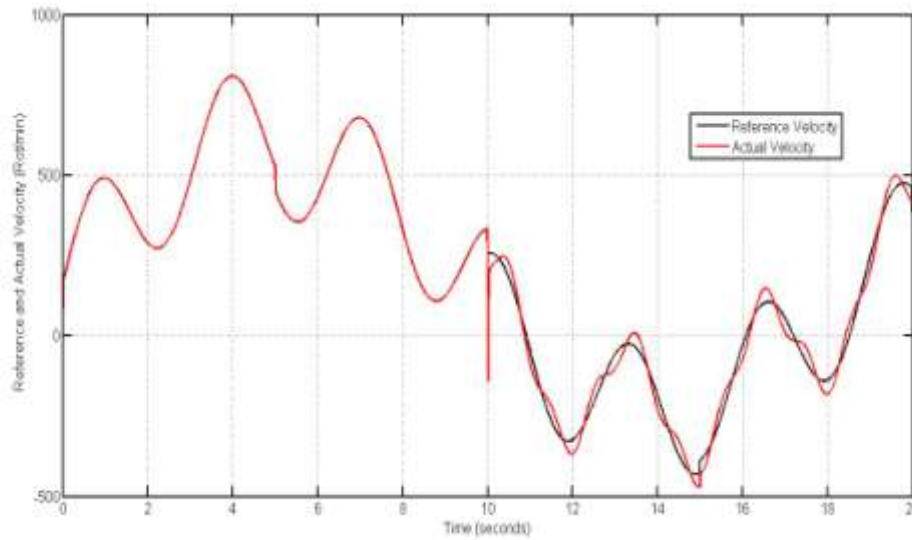


Figure 14: Effect of changing the external disturbance as in 23 for sinusoidal reference signal tracking.

As seen from Fig. 15, increasing the amplitude of disturbance spoils the performance slightly but the controller can still track the reference signal. As a last simulation, the effect of increasing the reference signal's frequency coupled with a pulse disturbance is monitored. In this application the reference signal is taken as:

$$r(t) = 200 \times \sin(20t) + 150 \times \sin(0.1t) + 400 \times (0.33t) + 1000 \times p(t) \text{ (rot/min)} \quad (24)$$

$r(t)$ in (24) includes a high frequency sinusoidal whose angular frequency is 20 rad/sec. Additionally an external constant torque of 0.1 Newton-meter is applied between 8th and 10th second as disturbance. Resulting voltage, current, velocity and external torque profiles are shown in Fig. 15.

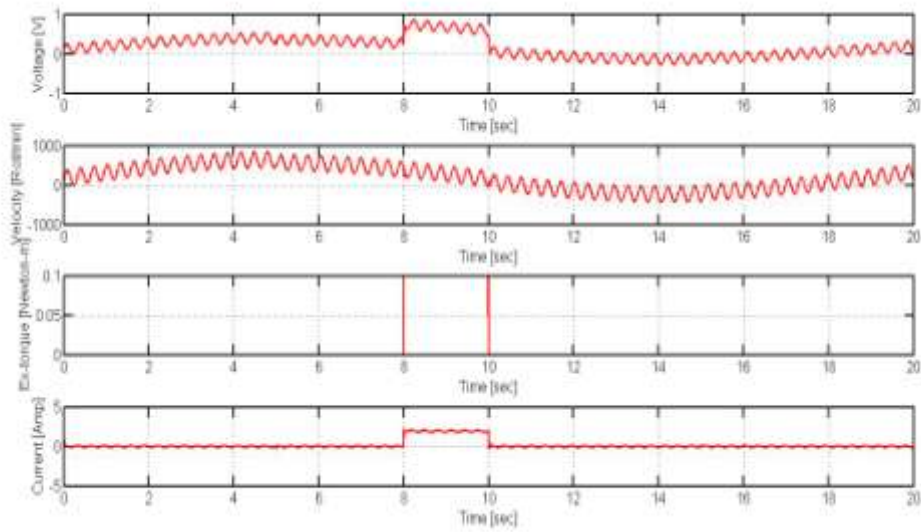


Figure 15: Voltage, velocity, external torque and current profiles in case of external square torque

To see the tracking performance of the controller more elaborately, both the reference signal and the actual velocity signal are drawn together in Fig. 16.

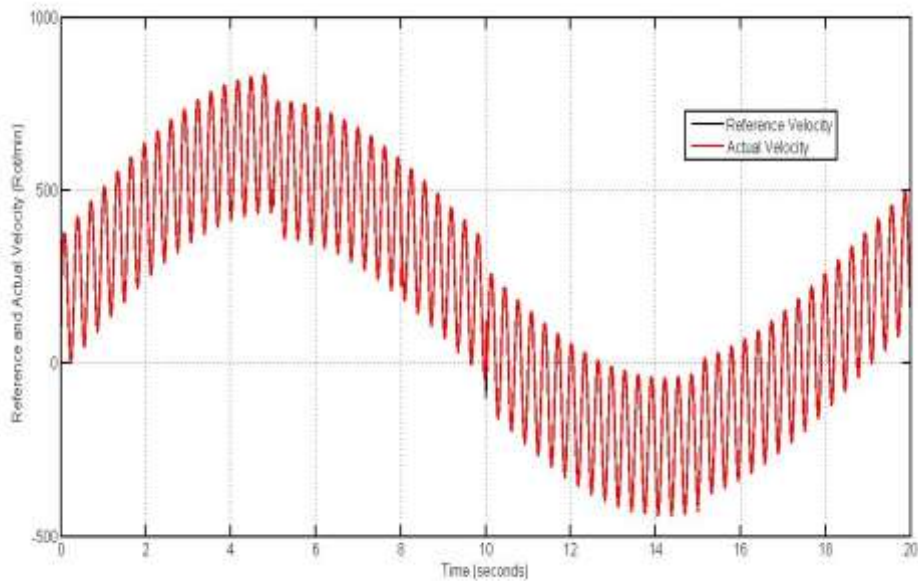


Figure 16: Reference signal and actual velocity signal in case of external square torque.

To have a better insight, Fig. 16 is redrawn with higher resolution in Fig. 17 to observe the effects of disturbance between 8th and 10th seconds

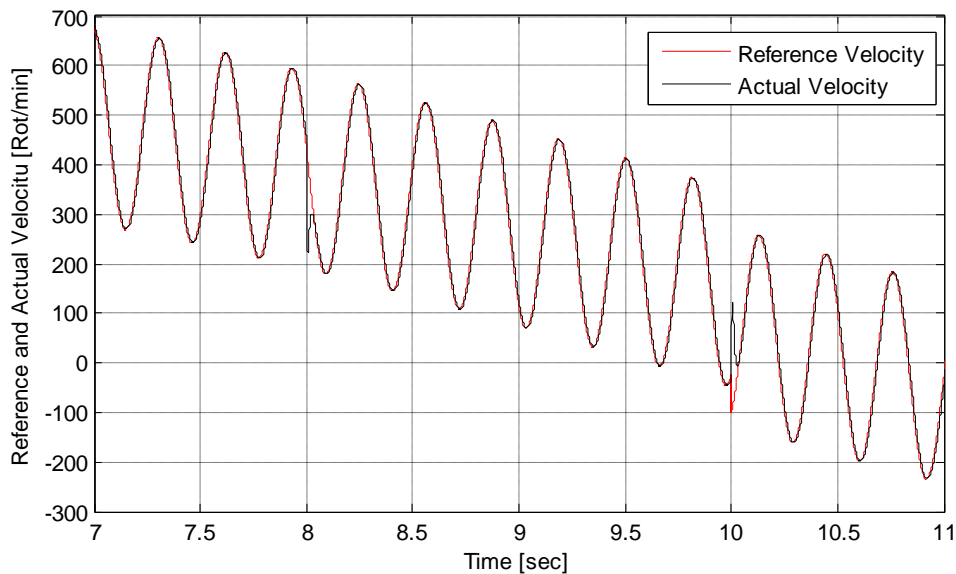


Figure 17: Reference signal and actual velocity signal drawn with higher resolution.

As seen from Fig. 18, the reference tracking task is nearly unspoiled except for the time instances that the disturbance pulse is just applied or removed as the motor react very rapidly to catch the reference signal. As seen from the simulation results, the obtained controller gives promising results at various scenarios with different reference signal and various disturbance load conditions and this controller structure is for this reason a good starting point for the motor to be controlled at real time applications.

V. CONCLUSION

In this study a methodology to provide a new controller structure that is applicable for a DC motor control system for controlling motor speed is proposed. This controller structure is then tested in various reference signal tracking and load disturbance conditions and it has been proved that the controller works very well in different simulation scenarios. This controller structure is supposed to be used as a starting point for real time applications. It will be used as a model and then if necessary some modifications will be done over the controller structure to make it more effective in the real time speed control application.

REFERENCES

- [1]. R. Bahador, E. Milad, R. Mohammad, Precise angular speed control of permanent magnet DC motors in presence of high modeling uncertainties via sliding mode observer-based model reference adaptive algorithm, *Mechatronics*, 28, 2015, 79–95.
- [2]. A. A. Sadiq, G. A. Bakare, E. C. Anene, H. B., Mamman, A fuzzy-based speed control of DC motor using combined armature voltage and field current, *Proc. 3rd IFAC International Conference on Intelligent Control and Automation Sciences*, Chengdu, China, 2013, 387–392.
- [3]. Y. Wenbin, W. Dada, J. Pengfei and L. Weiguo, The PWM speed regulation of DC motor based on intelligent control, *Systems Engineering Procedia*, 3, 2012, 259–267.
- [4]. K. Premkumar, B. V. Manikandan Adaptive neuro-fuzzy inference system based speed controller for brushless DC motor, *Neurocomputing*, 138, 2014, 260–270.
- [5]. S. Lekhchine, T. Bahil, I. Aadlia, Z. Layate, H. Bouzeria, Speed control of doubly fed induction motor, *Energy Procedia*, 74, 2015, 575–586.
- [6]. K. Premkumar, B. V. Manikandan, Fuzzy PID supervised online ANFIS based speed controller for brushless DC motor, *Neurocomputing*, 157, 2015, 76–90.
- [7]. C. P. Singh, S. Kulkarni, S. C. Rana, State-space based simulink modeling of BLCD motor and its speed control using fuzzy PID controller, *International Journal of Advances in Engineering Science and Technology*, 2(3) 2013, 359–369.
- [8]. A. A. Bohari, W. M. Utoma, Z. A. Haron, N. M. Zin, S. Y. Sim, R. M. Ariff, Speed tracking of indirect field oriented control induction motor using neural network, *Procedia Technology*, 11, 2013, 141–146.
- [9]. T. H. dos Santos., A. Goedel, S. A. O. da Silva, M. Suetake, Scalar control of an induction motor using a neural sensorless technique, *Electric Power Systems Research*, 108, 2014, 322–330.
- [10]. E. S. Ali, Speed control of induction motor supplied by wind turbine via Imperialist Competitive Algorithm, *Energy*, 89, 2015, 593–600.
- [11]. N. Öztürk, E. Çelik, Speed control of permanent magnet synchronous motors using fuzzy controller based on genetic algorithms, *Electrical Power and Energy Systems*, 43(1), 2012, 889–898.
- [12]. B. Bhushan, M. Singh, Adaptive control of DC motor using bacterial foraging algorithm, *Applied Soft Computing*, 11(8.) 2011, 4913–4920.
- [13]. S. Cao, J. Tub, Double Motor Coordinated Control Based on Hybrid Genetic Algorithm and CMAC, *Physics Procedia*, 33, 2012, 975–982.

- [14]. D. Fister, I. Fister Jr, I. Fister, R. Safaric, Parameter tuning of PID controller with reactive nature-inspired algorithms, *Robotics and Autonomous Systems*, 84, 2016, 64–75.
- [15]. E. Buzi, P. Marango, A Comparison of conventional and nonconventional methods of DC motor speed control, 15th Workshop on International Stability, Technology and Culture, Prishtina, Kosova, 2013, 50-53.
- [16]. R. C. Dorf, R. H. Bishop, *Modern control systems* (Upper Saddle River, NJ: Pearson-Prentice Hall, 2011).
- [17]. K. Ogata, *Modern control engineering*, (Upper Saddle River, NJ: Pearson-Prentice Hall, 2010).
- [18]. Precision modular servo control experiments manual 3-927, (East Sussex, United Kingdom: Feedback Instruments Ltd, 2013)

Ulas Beldek" Model Based PI Controller Design and Test of a DC Motor Using Root Locus"
International Journal of Engineering Science Invention (IJESI), Vol. 08, No. 05, 2019, PP 58-69